Radiological Physics and Technology (2019) 12:249–259
https://doi.org/10.1007/s12194-019-00515-9

# Evaluation of a new commercial automated planning software for tangential breast intensity-modulated radiation therapy

**Norifumi Mizuno[1,2] · Ryouhei Yamauchi[1] · Jiro Kawamori[1] · Tomoko Itazawa[1] · Munefumi Shimbo[2] · Keiichiro Nishimura[2] · Takafumi Yamano[2] · Shogo Hatanaka[1,2] · Masatsugu Hariu[2] · Takeo Takahashi[2]**

Received: 27 October 2018 / Revised: 15 May 2019 / Accepted: 17 May 2019 / Published online: 21 May 2019


**Abstract**
Automated treatment planning may decrease the effort required in planning and promote increased routine clinical use of intensity-modulated radiation therapy (IMRT) for many breast cancer patients. The aim of this study was to evaluate a new commercial automated planning software for tangential breast IMRT by comparing it with clinical plans from whole-breast irradiation. We prospectively enrolled 150 patients with Stage 0–1 breast cancer who underwent breast-conserving surgery at our institution between September 2016 and August 2017. Total doses of 42.56 Gy in 16 fractions ($n=98$) or 50 Gy in 25 fractions ($n=44$) were used. All treatment plans were retrospectively re-planned using the automated breast planning (ABP) software. All automated plans generated clinically deliverable beam parameters with no patient body collision and no contralateral breast pass through. The mean homogeneity index of the automatically generated clinical target volume, percentage volume of lungs receiving dose more than 20 Gy, mean heart dose, and dose to the highest irradiated 2-cc volumes of the irradiated volume were $0.077 \pm 0.019$, $4.2\% \pm 1.2\%$, $142 \pm 69$ cGy, and $105.8\% \pm 1.7\%$ (prescribed dose: 100%), respectively. The mean planning time was $4.8 \pm 1.4$ min. The ABP software demonstrated high clinical acceptability and treatment planning cost efficiency for tangential breast IMRT. The ABP software may be useful for delivering high-quality treatment to a majority of patients with early-stage breast cancer.

**Keywords** Automated treatment planning · Breast cancer · Whole-breast irradiation · Intensity-modulated radiation therapy

## 1 Introduction

Whole-breast irradiation (WBI) after breast-conserving surgery (BCS) is the standard for reducing local recurrence in patients with early-stage breast cancer [1–4]. More recently, intensity-modulated radiation therapy (IMRT) has been used to improve target dose homogeneity and reduce the organ at risk (OAR) dose in WBI. Several randomized studies have demonstrated that breast IMRT reduces acute toxicities relative to those of conventional radiation therapy using a physical wedge technique [5–8]. These results suggest that breast IMRT for WBI should be implemented after BCS. However, more planning time and expertise are often required to implement breast IMRT than to implement conventional treatment techniques. Our institution already applies the forward-planned IMRT technique in all WBI patients; consequently, the planning time has increased. Hence, automated treatment planning may promote greater use of breast IMRT in routine clinical practice without increasing the burden on clinical staff.

Automated planning for breast IMRT has been implemented in several institutions using in-house programs and/or their original scripting language for radiation treatment planning systems, although there were differences in the modules and degree of automation [9–13]. Recently, commercial automated breast planning (ABP) software from RayStation (version 4.7.4.4; RaySearch Laboratories, Stockholm, Sweden) was released. The ABP software was advertised as a fully automated solution that provided

**Electronic supplementary material** The online version of this article (https://doi.org/10.1007/s12194-019-00515-9) contains supplementary material, which is available to authorized users.

✉ Norifumi Mizuno
mizunono@luke.ac.jp

[1] Department of Radiation Oncology, St. Luke's International Hospital, 9-1 Akashi-cho, Chuo-ku, Tokyo 104-8560, Japan

[2] Department of Radiation Oncology, Saitama Medical Center, Saitama Medical University, 1981 Kamoda, Kawagoe City, Saitama 350-8550, Japan

segmentation of the relevant structures, localization of beam isocenters, determination of gantry and collimator angles, optimization of beam modulation, dose calculation, and plan reporting. However, the performance of commercial ABP software has not been reported for Asian patients. Moreover, previous studies of automated breast planning were performed using 6 MV and 18 MV photons only for patients in North America [9, 11, 13].

The purpose of this study was to evaluate the ABP software for Asian patients. Automated plans were generated using clinical CT images from WBI patients at our institution. Furthermore, the automated plans were compared with clinical treatment plans produced through standard manual planning in terms of beam parameters, dose–volume data, and planning time.

## 2 Materials and methods

### 2.1 Study population

We enrolled selected Stage 0–1 breast cancer patients who received BCS at our institution from September 2016 to August 2017. A total of 150 Asian patients were prospectively enrolled. The study protocol was approved by our institutional review board, and informed consent was obtained from all the patients before the computed tomography (CT) simulation of radiation treatment planning because the ABP software of RayStation required specific CT acquisition using radio-opaque markers and a radio-opaque wire. Eight patients were excluded from the analysis because they required a treatment course different from WBI ($n=6$) or declined to participate in this study ($n=2$). The clinical treatment plans specified a total dose of 42.56 Gy in 16 fractions ($n=98$) or 50 Gy in 25 fractions ($n=44$). A Varian Clinac 21EX (Varian Medical Systems, Inc., Palo Alto, CA, USA) with an 80-leaf Millennium multileaf collimator (MLC) was selected as the treatment instrument for 4 MV X-ray plans ($n=128$), and a Varian Clinac iX with a 120-leaf Millennium MLC was selected for 6 MV plans ($n=14$). Table 1 details the characteristics of the patient population and clinical plans. A total of 142 clinical plans were retrospectively re-planned using the ABP software and same planning CT images.

**Table 1** Characteristics of the patient population

| Parameter | *n* |
|---|---|
| *Breast side* | |
| Right | 74 (52%) |
| Left | 68 (48%) |
| *Age* | |
| ≥ 70 | 5 (4%) |
| ≥ 60, < 70 | 26 (18%) |
| ≥ 50, < 60 | 36 (25%) |
| ≥ 40, < 50 | 61 (43%) |
| ≥ 30, < 40 | 13 (9%) |
| < 30 | 1 (1%) |
| *Area* | |
| *A* | 26 (18%) |
| *B* | 8 (6%) |
| *C* | 93 (65%) |
| *D* | 11 (8%) |
| *E* | 3 (2%) |
| *C'* | 1 (1%) |
| *BMI* | |
| ≥ 27.5, < 30 | 1 (1%) |
| ≥ 25, < 27.5 | 13 (9%) |
| ≥ 22.5, < 25 | 31 (22%) |
| ≥ 20, < 22.5 | 52 (37%) |
| ≥ 17.5, < 20 | 36 (26%) |
| ≥ 15, < 17.5 | 7 (5%) |
| *Prescription dose* | |
| 42.56 Gy/16 fr. | 98 (69%) |
| 50 Gy/25 fr. | 44 (31%) |
| *X-ray energy* | |
| 4 MV | 128 (90%) |
| 6 MV | 14 (10%) |

*BMI* body mass index

### 2.2 CT simulation

The CT simulations were performed assuming that ABP would be used. A Lightspeed RT16 CT scanner (GE Healthcare, Waukesha, WI, USA) was used to capture images at a slice thickness of 2.5 mm. The simulation was performed with a patient lying supine on a Wing Support (Engineering System Co., Ltd., Matsumoto, Nagano, Japan) with both arms raised above the head (Fig. 1). Four radio-opaque markers and a radio-opaque wire were placed on the patient as recommended by RaySearch Laboratories and described in the RayStation user manual [14].

### 2.3 Clinical treatment planning

The RTPS Pinnacle$^3$ (version 9.10, Philips Radiation Oncology Systems, Fitchburg, WI, USA) was used for clinical treatment planning by three experienced breast radiation oncologists certified by the Japanese Society for Radiation Oncology (JASTRO). Forward-planned IMRT plans that comprised two tangential field-in-field (FIF) beams with a matched posterior by gantry-tilting technique without half-beam technique were generated (Fig. 2). Lung and heart sparing were performed using MLC shielding without using collimator rotation (i.e., collimator rotation: 0 degrees).

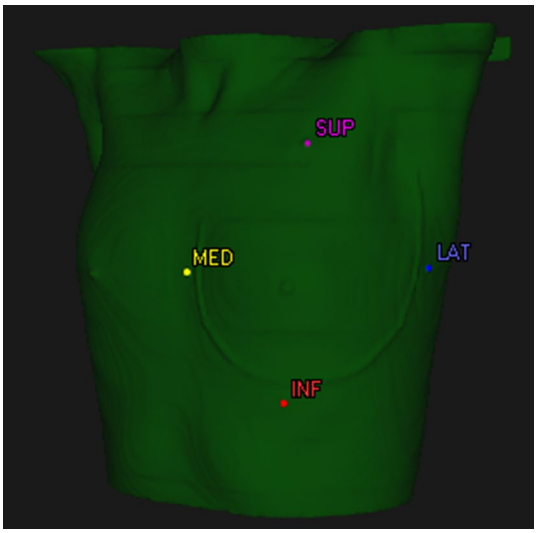


**Fig. 1** Example of CT simulation with four radio-opaque markers and a radio-opaque wire on the surface of the patient. *SUP* superior marker, *INF* inferior marker, *LAT* lateral marker, *MED* medial marker. A radio-opaque wire was placed around the breast tissue

The planner provided manual definitions of the mammary gland as the clinical target volume (CTV), lungs, and heart in accordance with the European Society for Radiotherapy and Oncology (ESTRO) consensus guidelines [15]. For dosimetric evaluation, the CTV for the evaluation (CTVeval) was defined as the volume of the CTV restricted to the tissue outside the first 5 mm of skin and lung–chest interface. A three-dimensional 1-cm margin (posterior side: 5 mm) was added to the CTV to obtain the planning target volume (PTV). The beam isocenters was set at the center of PTV. A skin flash was performed by opening the X-JAW 2–3 cm from the skin to account for swelling of the breast or respiratory motion. The grid size for dose calculation was set to a constant value of 2 mm and an adaptive convolve algorithm with heterogeneity correction was performed. Reference point positions within CTV were optimized manually to accomplish ICRU 62 recommendations regarding homogeneous target coverage (95–107% of the prescribed dose); coverage of the PTV by at least 90% of the prescription dose was encouraged [16]. However, the above criteria were not met in all patients because our facility had performed aggressive heart shielding for the reduction of the heart dose in exchange for coverage of the PTV.

## 2.4 Automated treatment planning

RayStation (version 4.7.4.4; RaySearch Laboratories, Stockholm, Sweden) ABP software was used. The software generates tangential breast or chest-wall IMRT plans using heuristic optimization [11]. Placement of the radio-opaque markers and radio-opaque wire during CT acquisition enables the algorithm to identify the breast or chest wall. First, automatic detection of the marker and wire is performed. Second, automatic segmentation is performed for the relevant target and OARs (e.g., breast or chest wall, lung, heart, humeral head, and dummy structures for the optimization of gantry and collimator angles). Two opposed half-beams with a skin flash were generated and, then, optimization of gantry angles, collimator angles, beam weighting of each segments, and step-and-shoot segmentation was performed automatically. Figure 3 shows a typical IMRT plan generated by the RayStation ABP software.

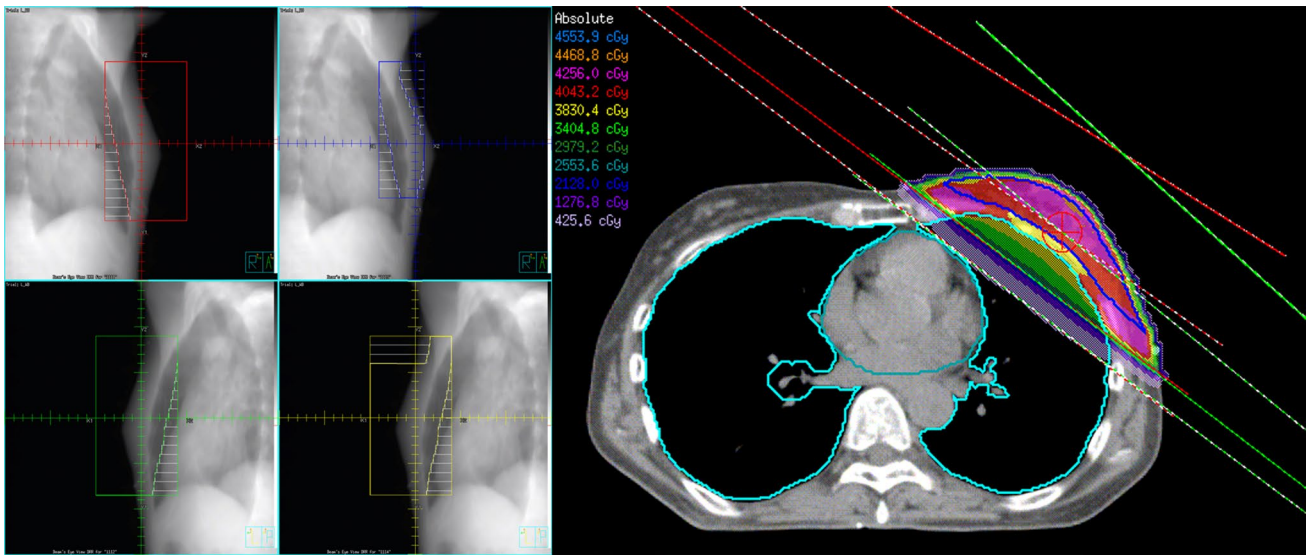


**Fig. 2** Left: Example of the typical MLC segments of a clinical plan from the point-of-view of the beam. Right: Example of the dose distribution in the clinical plan (left-sided WBI, prescription of 42.56 Gy/16 fr.)

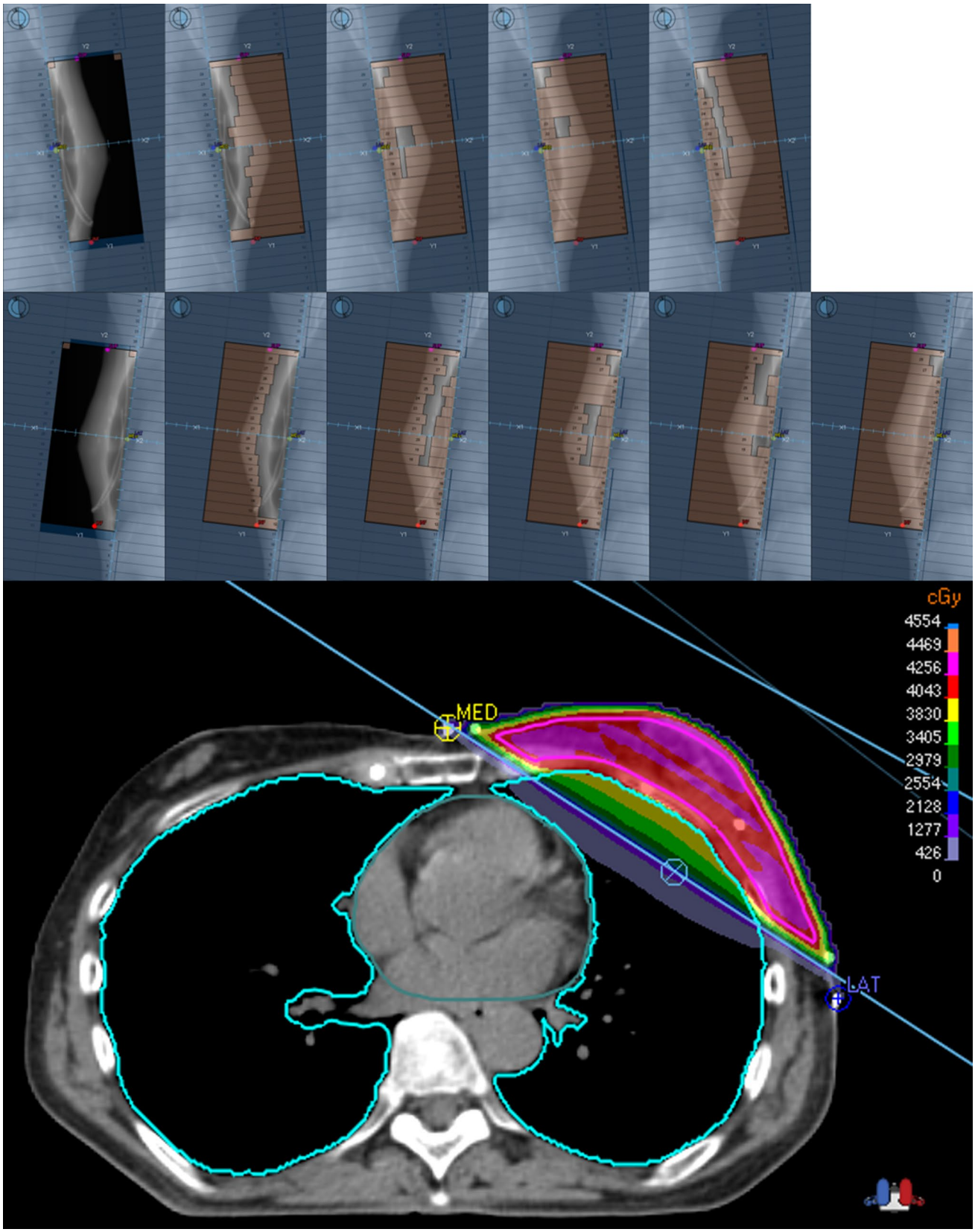


**Fig. 3** Top: Example of the typical MLC segments of an automated plan from the point-of-view of the beam. Bottom: Example of the dose distribution in the automated plan (left-sided WBI, prescription of 42.56 Gy/16 fr.)

Whole-breast and breast-coverage modes from the default planning parameters in the ABP settings were used [14]. The advanced settings of ABP software were not used (e.g., optional optimization of a manually defined cavity) in generating the plans. Manual definition of the marker position was not performed (i.e., automatic detection only), and the optimization was not continued after generating the initial plans. Since this software automatically sets the isocenter from the imported CT images, the isocenter set during CT simulation cannot be applied for plan isocenter without manual point definition. The average dose ($D_{average}$) prescription was performed for an automatically generated clinical target volume (aCTV) for WBI at a normal setting of ABP software. The grid size for dose calculation was set to a constant value of 2 mm. Collapsed cone convolution with heterogeneity correction was used as the dose calculation algorithm.

### 2.5 Beam parameter comparison

Beam parameters were evaluated for their usefulness in clinically possible geometric configurations (e.g., no collision with a patient or a treatment bed). For all clinical plans and automated plans, the beam parameters of isocenter location, gantry angle, collimator angle, and JAW size for each beam were recorded. The number of segments and total monitor units (MUs) as well as the MUs of open segments were recorded for each plan.

### 2.6 Dose–volume data comparison

Ninety percent of prescribed dose–volume overlap between clinical plans and automated plans was evaluated using the dice similarity coefficient (*DSC*) and Hausdorff distance using 3D Slicer software (version 4.6.0, http://www.slicer.org, [17]). Dose–volume data regarding the homogeneity index (*HI*) of CTV (CTVeval for clinical plans and aCTV for automated plans), percentage volume of manually defined lungs receiving dose greater than 20 Gy ($V_{20\,Gy}$), mean dose ($D_{mean}$) of the manually defined heart (left-sided breast only), and dose to the most highly irradiated 2 cc volumes ($D_{2\,cc}$) of the irradiated volume were recorded. *HI* was calculated per the following equation from the ICRU 83 recommendation [18]:

$$\mathrm{HI} = \left(D_{2\%} - D_{98\%}\right)/D_{50\%}, \tag{1}$$

where $D_{x\,\%}$ is the absorbed dose received by $x\%$ of the volume. Manually defined structures (i.e., heart and lungs) were imported from each clinical plan that was contoured by three experienced breast radiation oncologists certified by JASTRO. In this dose–volume data comparison, manually defined OAR structures were dealt with as "gold standard," although automated defined structures were generated by ABP software.

### 2.7 Statistical analysis

Data were analyzed using R software (version 3.4.1, R Foundation for Statistical Computing, Vienna, Austria). A paired *t* test was used for comparisons between clinical plans and automated plans, with $P < 0.05$ considered to be significant.

### 2.8 Planning time

The planning time was recorded using a hand timer from the time of immediately importing CT images to the end of the plan evaluation of each plan by three experienced breast radiation oncologists certified by the JASTRO.

### 2.9 Clinical acceptability

Automated plans were evaluated regarding clinical acceptability by three experienced breast radiation oncologists certified by JASTRO. Each of the plans was evaluated according to dose coverage and homogeneity to the target, dose of critical organs and presence or absence of hot spot in the irradiated volume from the view point of ICRU 62 and 83 recommendations, ESTRO consensus guidelines, and American Society for Radiation Oncology (ASTRO) evidence-based guidelines [15, 16, 18, 19].

## 3 Results

### 3.1 Beam parameter comparison

The comparison between beam parameters of clinical and automated plans are shown in Table 2. For the gantry angle of the right-sided breasts in automated plans, the means ± standard deviations (range) of the medial and lateral beams were 55.3° ± 4.3° (42.0°–63.0°) and 235.3° ± 4.3° (222.0°–243.0°), respectively. In the left-sided breast of automated plans, the gantry angles of the medial and lateral beams were 305.5° ± 4.8° (292.0°–316.0°) and 125.5° ± 4.7° (114.0°–136.0°), respectively. In all automated plans, the half-beams were generated with single isocenters as opposed to matched fields. Of the 284 beams in automated plans, most beams were generated with a collimator rotation of approximately 8° to 9° (8.6° ± 3.5° [5.0°–20.0°]). The JAW sizes of the *X* and *Y* directions were 8.1 ± 1.0 cm (5.5–12.3 cm) and 18.3 ± 1.6 cm (14.8–23.3 cm), respectively, for the 284 beams in automated plans. For the isocenter location, most automated plans were generated within 1 cm of clinical plans except for the posterior-to-anterior direction (supplemental data; appendix A). For the gantry angle, most automated plans were generated within 5° of clinical plans (supplemental data; appendix B). For the JAW opening,

**Table 2** Comparison of beam parameters of the clinical plans and automated plans

| Parameter | *n* | Clinical plans | Automated plans | *p* |
|---|---|---|---|---|
| Gantry angle | | | | |
| Right-sided breast | | | | |
| Medial beam | 74 | 56.6 ± 4.0 [45.0–65.0] | 55.3 ± 4.3 [42.0–63.0] | < 0.001 |
| Lateral beam | 74 | 232.8 ± 4.1 [221.0–241.0] | 235.3 ± 4.3 [222.0–243.0] | 0.002 |
| Left-sided breast | | | | |
| Medial beam | 68 | 304.0 ± 4.7 [293.0–315.0] | 305.5 ± 4.8 [292.0–316.0] | < 0.001 |
| Lateral beam | 68 | 127.6 ± 4.9 [116.0–139.0] | 125.5 ± 4.7 [114.0–136.0] | < 0.001 |
| Collimator angle | | | | |
| Right-sided breast | | | | |
| Medial beam | 74 | – | −8.1 ± 3.3 [− 20.0–5.0] | – |
| Lateral beam | 74 | – | 8.1 ± 3.3 [5.0–20.0] | – |
| Left-sided breast | | | | |
| Medial beam | 68 | – | 9.0 ± 3.6 [5.0–20.0] | – |
| Lateral beam | 68 | – | −8.9 ± 3.7 [− 20.0–5.0] | – |
| JAW opening (cm) | | | | |
| Medial beam | | | | |
| X-JAW | 142 | 10.0 ± 1.1 [7.5–13.5] | 8.1 ± 1.0 [5.5–12.3] | < 0.001 |
| Y-JAW | 142 | 17.3 ± 1.5 [14.5–21.0] | 18.3 ± 1.6 [14.8–23.3] | < 0.001 |
| Lateral beam | | | | |
| X-JAW | 142 | 10.0 ± 1.1 [7.5–13.7] | 8.1 ± 1.0 [5.5–12.3] | < 0.001 |
| Y-JAW | 142 | 17.3 ± 1.5 [14.5–21.0] | 18.3 ± 1.6 [14.8–23.3] | < 0.001 |
| Number of segments/plan | | | | |
| 42.56 Gy/16 fr. | 98 | 4.7 ± 1.2 [2.0–10.0] | 10.4 ± 1.5 [7.0–14.0] | < 0.001 |
| 50 Gy/25 fr. | 44 | 4.4 ± 0.8 [3.0–6.0] | 9.0 ± 1.2 [6.0–12.0] | < 0.001 |
| Total MUs/plan | | | | |
| 42.56 Gy/16 fr. | 98 | 322.6 ± 12.9 [290.0–357.0] | 360.4 ± 11.1 [332.0–387.6] | < 0.001 |
| 50 Gy/25 fr. | 44 | 242.8 ± 9.1 [225.0–261.0] | 268.1 ± 8.5 [248.4–284.6] | < 0.001 |
| MUs of open segment/beam | | | | |
| 42.56 Gy/16 fr. | 196 | 142.8 ± 8.2 [115.9–162.6] | 142.1 ± 4.4 [130.6–156.4] | 0.329 |
| 50 Gy/25 fr. | 88 | 107.8 ± 4.9 [92.0–120.0] | 107.1 ± 3.2 [99.3–115.9] | 0.301 |
| Weight of open segment/beam (%) | 284 | 88.8 ± 4.8 [73.2–100.0] | 79.3 ± 3.3 [68.8–88.5] | < 0.001 |

Values are presented as the mean ± standard deviation [range]

*MUs* monitor units

most automated plans were approximately 2 cm smaller in the *X* direction and 1 cm larger in the *Y* direction than clinical plans (supplemental data; appendix C).

Most automated plans were generated with nine to ten segments (prescription of 42.56 Gy: 10.4 ± 1.5 [7.0–14.0]; prescription of 50 Gy: 9.0 ± 1.2 [6.0–12.0]), and total MUs approximately 10% larger than clinical plans (prescription of 42.56 Gy: 360.4 ± 11.1 [332.0–387.6]; prescription of 50 Gy: 268.1 ± 8.5 [248.4–284.6]). Most of the beams in automated plans were generated with an open segment that was weighted to approximately 80% of the beam MUs (79.3% ± 3.3% [68.8%–88.5%]). All beam parameters had significant differences between clinical plans and automated plans except the MUs of open segments.

## 3.2 Dose–volume data comparison

Figure 4 shows the distribution of *DSC* and Hausdorff distance regarding the 90% dose–volume between clinical plans and automated plans. *DSC* was 0.80–0.90 in most patients (0.84 ± 0.05 [0.70–0.93]). However, there were several patients with a maximum Hausdorff distance > 3 cm. The volume was not significantly different between clinical plans and automated plans (clinical plans: 684.8 ± 251.0 $cm^3$ [261.1–1401.7 $cm^3$]; automated plans: 689.9 ± 261.1 $cm^3$ [243.1–2050.6 $cm^3$; $P = 0.674$]).

Table 3 shows the analysis of dose–volume data for the target and relevant structures. The mean *HI* values of CTV for clinical plans and automated plans were

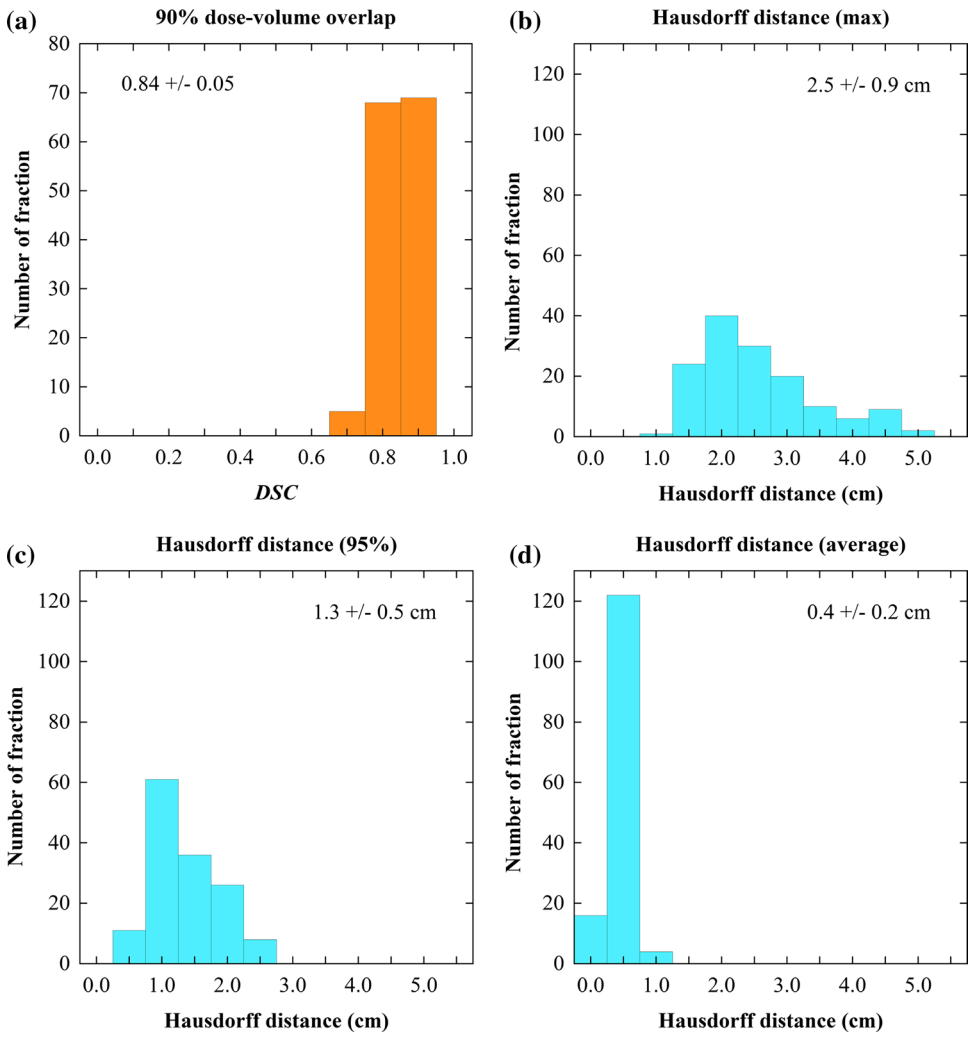


**Fig. 4** Distribution of 90% dose-volume overlap between the clinical plans and automated plans ($n = 142$). **a** Dice similarity coefficient (*DSC*). **b** Maximum Hausdorff distance. **c** 95% Hausdorff distance. **d** Average Hausdorff distance

$0.110 \pm 0.031$ and $0.078 \pm 0.019$, respectively, indicating that, on average, the CTV dose in automated plans was more homogeneous ($P < 0.001$). The $V_{20Gy}$ value for manually defined lungs of automated plans (prescription of 42.56 Gy: $4.2\% \pm 1.2\%$ [1.3%–8.3%]; prescription of 50 Gy: $4.3\% \pm 1.3\%$ [2.0%–7.0%]) was significantly lower ($P < 0.001$) than the value in clinical plans (prescription of 42.56 Gy: $5.1\% \pm 2.0\%$ [0.7%–10.5%]; prescription of 50 Gy: $6.0\% \pm 2.5\%$ [1.5%–11.5%]). A significantly higher $D_{mean}$ value for the manually defined hearts ($P < 0.001$) was found with automated plans (prescription of 42.56 Gy: $141 \pm 72$ cGy [62–433 cGy]; prescription of 50 Gy: $146 \pm 64$ cGy [66–291 cGy]) compared with that of the clinical plans (prescription of 42.56 Gy: $91 \pm 21$ cGy [58–143 cGy]; prescription of 50 Gy: $103 \pm 21$ cGy [69–151 cGy]). The differences between clinical plans and automated plans for $D_{2\ cc}$ values of the irradiated volume were not found to be significant (prescription of 42.56 Gy: $P = 0.548$) or small (prescription of 50 Gy: $P = 0.017$).

## 3.3 Planning time

The mean planning time of automated plans (4.8 min ± 1.4 min [3.5 min–7.8 min]) was significantly shorter ($P < 0.001$) than that of clinical plans (53.1 min ± 6.7 min [40.0 min–70.0 min]).

## 3.4 Clinical acceptability

Table 4 shows the clinical acceptability of automated plans as evaluated by three experienced radiation oncologists; 136 (95.8%) automated plans were deemed to be clinically usable. Conversely, six (4.2%) automated plans were rejected due to the coverage of target volume ($n = 2$, 1.4%) or high heart dose ($n = 4$, 2.8%).

**Table 3** Analysis of dose–volume data for the target and relevant structures in the automated plans

| Parameter | *n* | Clinical plans | Automated plans | *p* |
|---|---|---|---|---|
| CTV | | | | |
| $D_{2\,\%}$ (cGy) | | | | |
| 42.56 Gy/16 fr. | 98 | 4493 ± 17 [4438–4527] (105.6 ± 0.4% [104.3–106.4]) | 4432 ± 52 [4349–4527] (104.1 ± 1.2% [102.2–106.4]) | < 0.001 |
| 50 Gy/25 fr. | 44 | 5278 ± 31 [5229–5419] (105.6 ± 0.6% [104.6–108.4]) | 5197 ± 55 [5098–5343] (103.9 ± 1.1% [102.0–106.9]) | < 0.001 |
| $D_{50\,\%}$ (cGy) | | | | |
| 42.56 Gy/16 fr. | 98 | 4324 ± 44 [4216–4413] (101.6 ± 1.0% [99.1–103.7]) | 4257 ± 16 [4245–4410] (100.0 ± 0.4% [99.7–103.6]) | < 0.001 |
| 50 Gy/25 fr. | 44 | 5079 ± 63 [4910–5192] (101.6 ± 1.3% [98.2–103.8]) | 5000 ± 4 [4994–5011] (100.0 ± 0.1% [99.9–100.2]) | < 0.001 |
| $D_{98\,\%}$ (cGy) | | | | |
| 42.56 Gy/16 fr. | 98 | 4013 ± 140 [3595–4218] (94.3 ± 3.3% [84.5–99.1]) | 4099 ± 33 [3994–4156] (96.3 ± 0.8% [93.8–97.7]) | < 0.001 |
| 50 Gy/25 fr. | 44 | 4736 ± 130 [4416–4938] (94.7 ± 2.6% [88.3–98.8]) | 4823 ± 33 [4723–4880] (96.5 ± 0.7% [94.5–97.6]) | < 0.001 |
| *HI* | | | | |
| 42.56 Gy/16 fr. | 98 | 0.111 ± 0.033 [0.068–0.214] | 0.078 ± 0.020 [0.047–0.132] | < 0.001 |
| 50 Gy/25 fr. | 44 | 0.107 ± 0.025 [0.070–0.176] | 0.075 ± 0.017 [0.044–0.121] | < 0.001 |
| Lung | | | | |
| $V_{20\mathrm{Gy}}$ (%) | | | | |
| 42.56 Gy/16 fr. | 98 | 5.1 ± 2.0 [0.7–10.5] | 4.2 ± 1.2 [1.3–8.3] | < 0.001 |
| 50 Gy/25 fr. | 44 | 6.0 ± 2.5 [1.5–11.5] | 4.3 ± 1.3 [2.0–7.0] | < 0.001 |
| Heart | | | | |
| $D_{\mathrm{mean}}$ (cGy) | | | | |
| 42.56 Gy/16 fr. | 49 | 91 ± 21 [58–143] | 141 ± 72 [62–433] | < 0.001 |
| 50 Gy/25 fr. | 19 | 103 ± 21 [69–151] | 146 ± 64 [66–291] | 0.006 |
| $V_{25\,\mathrm{Gy}}$ (%) | | | | |
| 42.56 Gy/16 fr. | 49 | 0.1 ± 0.2 [0.0–0.7] | 1.2 ± 1.4 [0.0–7.0] | < 0.001 |
| 50 Gy/25 fr. | 19 | 0.1 ± 0.2 [0.0–0.9] | 0.9 ± 1.0 [0.0–3.4] | 0.002 |
| Irradiated volume | | | | |
| $D_{2\,\mathrm{CC}}$ (cGy) | | | | |
| 42.56 Gy/16 fr. | 98 | 4518 ± 20 [4460–4624] (106.2 ± 0.5% [104.8–108.6]) | 4514 ± 75 [4378–4706] (106.1 ± 1.8% [102.9–110.6]) | 0.548 |
| 50 Gy/25 fr. | 44 | 5307 ± 30 [5252–5424] (106.1 ± 0.6% [105.0–108.5]) | 5277 ± 81 [5126–5471] (105.5 ± 1.6% [102.5–109.4]) | 0.017 |

Values are presented as the mean ± standard deviation [range]

*D* dose, *HI* homogeneity index, *V* volume

## 4 Discussion

This study confirmed that the RayStation ABP software generated clinically deliverable beam parameters in all plans. The automated plans using a half-beam technique located the isocenter on the posterior side of the patients compared with clinical plans using a gantry-tilting technique. Although there were significant differences between clinical plans and automated plans regarding all beam parameters, except the MUs of open segments, the tangential gantry angles of automated plans were generated within a range that is frequently used in clinical WBI without collision with the patient and without passing through the contralateral breast or treatment bed [20–22]. The collimator angles were selected to provide efficient shielding for the lungs without inefficient MLC sequences due to excessive rotation and without inefficient JAW sizes [9]. The Y-JAW opening of automated plans was increased from the opening of clinical plans; this was caused by ensuring target coverage even with the rotation of the collimators. Conversely, the X-JAW opening of automated plans was decreased from the opening of clinical plans. This may have been caused by ABP software systematically

**Table 4** Clinical acceptability of automated plans

| Parameter | *n* |
|---|---|
| Clinically acceptable | 136 (95.8%) |
| Comment of radiation oncologist | |
| Excellent | 95 (66.9%) |
| Average | 40 (28.2%) |
| Poor | 1 (0.7%) |
| Clinically unacceptable | 6 (4.2%) |
| Reason of clinically unacceptable | |
| Plan 43: Coverage of target volume (medial side) | |
| Plan 52: Heart dose ($D_{mean}$ of heart: 198 cGy) | |
| Plan 64: Coverage of target volume (medial side) | |
| Plan 68: Heart dose ($D_{mean}$ of heart: 238 cGy) | |
| Plan 112: Heart dose ($D_{mean}$ of heart: 433 cGy) | |
| Plan 118: Heart dose ($D_{mean}$ of heart: 213 cGy) | |

$D_{mean}$, mean dose

performing a skin flash by opening the X-JAW 2 cm from the skin without variation due to manual selection performed by the planners. The number of segments and total MUs that the automated plans used were the same as those used in a previous study [11]. Most of the open segments of automated plans were generated with a similar MU to that of clinical plans. Moreover, several previous studies mentioned that the weight of the open segment, like in this study, may provide a highly robust plan to account for uncertainty in the patient setup and respiratory motion [23, 24]. The RayStation ABP software is based on the Pinnacle$^3$ (Philips Radiation Oncology Systems, Fitchburg, WI, USA) original language and Python scripting that was developed using a subset of analyzed clinical plans at Princess Margaret Hospital for the patients in North America [11]. Consequently, the software's heuristic approach demonstrated clinical utility even when the software platform was changed to RayStation and has been applied to Asian patients.

Dose–volume data were evaluated for the 90% dose–volume overlap, target, and OARs between clinical plans and automated plans. The *DSC* and volume of the 90% dose–volume showed good agreement between clinical plans and automated plans, although the Hausdorff distance showed a local deviation caused by the presence or absence of collimator rotation. The target dose was more homogeneous for automated plans than for clinical plans because of the intensity modulation when using a smaller size of segmentation and a larger number of segments. The mean dose homogeneity of CTV was 7.7% for automated plans, which was similar to that of a previous report for the tangential breast IMRT technique, even when the beam energy was 4 MV and the beam modifier was an 80-leaf Millennium MLC for Asian patients [11]. The mean maximum dose using $D_{2cc}$ was approximately 104% at the CTV and approximately 106% at the irradiated volume (prescribed dose: 100%) in automated plans. Since a high dose > 105% of the prescription dose at the irradiated volume was not observed in the breast tissue or OARs in most plans, the plan would be clinically acceptable [19]. The lung dose was evaluated using the $V_{20Gy}$ value for lungs, and the dose for automated plans was significantly smaller than that for clinical plans. Although the lung dose was evaluated ipsilaterally in a previous study, the $V_{20Gy}$ of the lungs in our study appeared to be similar and the dose levels were acceptable [11, 25]. In particular, half-beam blocking and collimator rotation were available to provide effective shielding of the lungs due to the lower transmission of the JAW collimator than that of the MLC. The heart doses were evaluated using the $D_{mean}$, with a mean value of approximately 142 cGy for automated plans. The heart dose in automated plans was significantly higher than that in clinical plans at our institution. We consider that the difference in the heart dose between automated plans and clinical plans was caused by aggressive heart shielding in exchange for coverage of the PTV at our facility. Recently, heart doses from modern breast radiation therapy have been reported in several studies [26–28]. According to a report from CW Taylor et al., the mean heart doses in left tangential breast cancer radiation therapy were 320–350 cGy in Japan [26]. Furthermore, Pierce et al. reported that the mean heart dose in a recent study of irradiation technique was 165 cGy at 20 sites in the United States [28]. Therefore, the heart dose in the automated plan of the present study will be clinically applicable in most cases. However, the $D_{mean}$ of the heart was > 200 cGy in three (2.1%) automated plans (213 cGy, 238 cGy, and 433 cGy). In such cases, manual definition of the marker position could adjust the plan to provide the optimum beam edge position and gantry angle for heart sparing.

Most automated plans (> 95%) were deemed clinically acceptable by the radiation oncologists, with the opinion that the plans had better dose distribution for the target and OARs. Six automated plans were rejected due to the coverage of target volume or high heart dose. As previously mentioned, those rejected plans seem likely to improve to acceptable plans by manual definition of the marker position for suitable gantry angle and JAW opening. The planning time when using the ABP software was approximately 5 min from the importing of the CT images to the end of the plan evaluation by a planner. In most cases, the automatic sequence of plan generation (i.e., segmentation of relevant structures, placement of beams, optimization of beams, dose calculation) was performed in 3.5 min. Generally, a tangential breast IMRT plan requires approximately 60 min of manual planning to be performed in the same manner as that in our institutions [9, 29]. Recently, the number of patients with early-stage breast cancer has increased worldwide [30, 31]. Therefore, the number and

rate of breast treatments have grown in radiation oncology departments [31, 32]. ABP software could dramatically decrease the planning time and improve planning efficiency for clinical sites that have a large number of breast cancer patients (e.g., saving ≥ 300 h per year in our institution).

This study evaluated the ABP software using a clinical CT data set from WBI. However, the actual dose delivery to patients was not performed. Additionally, the "chest wall" planning setting of the ABP software for post-mastectomy radiation therapy (PMRT) was not validated. The ABP software forces collimator rotation in all beams and a supraclavicular field for PMRT is not generated. It is notable that this version (v4.7.4.4) of the ABP software does not correspond to the clinical requirement of creating a single isocenter PMRT plan with a supraclavicular field using half-beam matching.

## 5 Conclusion

We performed the first evaluation of a new commercial ABP software for tangential breast IMRT by comparing it with clinical treatment plans. We found that the RayStation ABP software generated clinically usable WBI plans for Asian patients. The beams of the automated plans were generated with no collision with the patient, no passing through the contralateral breast, and with high robustness to accommodate the uncertainty in patient setup. The dose homogeneity of the target was satisfactory, and the OAR dose level was acceptable. The time cost of planning was dramatically improved. Use of the RayStation ABP software may enable high-quality WBI using tangential IMRT technique for a large number of patients.

**Acknowledgements** Some of the findings reported here were presented at The 30th Annual Meeting of the Japanese Society for Radiation Oncology in Osaka-shi, Osaka-fu, Japan, held November 17–19, 2017.

### Compliance with ethical standards

**Conflict of interest** The authors declare that there are no conflicts of interest.

**Ethical approval** All procedures performed in studies involving human participants were in accordance with the ethical standards of the institutional review board and with the 1964 Helsinki declaration and its later amendments or comparable ethical standards.

**Statement of animal rights** This article does not contain any studies with animals performed by any of the authors.

**Informed consent** Informed consent was obtained from all individual participants included in the study.

## References

1. Clark RM, Whelan T, Levine M, Roberts R, Willan A, McCulloch P, Lipa M, Wilkinson RH, Mahoney LJ. Randomized clinical trial of breast irradiation following lumpectomy and axillary dissection for node-negative breast cancer: an update. Ontario Clinical Oncology Group. J Natl Cancer Inst. 1996;20:1659–64.
2. Veronesi U, Cascinelli N, Mariani L, Greco M, Saccozzi R, Luini A, Aguilar M, Marubini E. Twenty-year follow-up of a randomized study comparing breast-conserving surgery with radical mastectomy for early breast cancer. N Engl J Med. 2002;347:1227–32.
3. Fisher B, Anderson S, Bryant J, Margolese RG, Deutsch M, Fisher ER, Jeong JH, Wolmark N. Twenty-year follow-up of a randomized trial comparing total mastectomy, lumpectomy, and lumpectomy plus irradiation for the treatment of invasive breast cancer. N Engl J Med. 2002;347:1233–41.
4. Darby S, McGale P, Correa C, Taylor C, Arriagada R, Clarke M, Cutter D, Davies C, Ewertz M, Godwin J, Gray R, Pierce L, Whelan T, Wang Y, Peto R. Effect of radiotherapy after breast-conserving surgery on 10-year recurrence and 15-year breast cancer death: meta-analysis of individual patient data for 10,801 women in 17 randomised trials. Lancet. 2011;378:1707–16.
5. Pignol JP, Olivotto I, Rakovitch E, Gardner S, Sixel K, Beckham W, Vu TT, Truong P, Ackerman I, Paszat L. A multicenter randomized trial of breast intensity-modulated radiation therapy to reduce acute radiation dermatitis. J Clin Oncol. 2008;26:2085–92.
6. Mukesh MB, Barnett GC, Wilkinson JS, Moody AM, Wilson C, Dorling L, Chan Wah Hak C, Qian W, Twyman N, Burnet NG, Wishart GC, Coles CE. Randomized controlled trial of intensity-modulated radiotherapy for early breast cancer: 5-year results confirm superior overall cosmesis. J Clin Oncol. 2013;31:4488–95.
7. Mukesh MB, Qian W, Wah Hak CC, Wilkinson JS, Barnett GC, Moody AM, Wilson C, Coles CE. The Cambridge Breast Intensity-modulated Radiotherapy Trial: comparison of clinician- versus patient-reported outcomes. Clin Oncol (R Coll Radiol). 2016;28:351–64.
8. Pignol JP, Truong P, Rakovitch E, Sattler MG, Whelan TJ, Olivotto IA. Ten years results of the Canadian breast intensity modulated radiation therapy (IMRT) randomized controlled trial. Radiother Oncol. 2016;121:414–9.
9. Vicini FA, Sharpe M, Kestin L, Martinez A, Mitchell CK, Wallace MF, Matter R, Wong J. Optimizing breast cancer treatment efficacy with intensity-modulated radiotherapy. Int J Radiat Oncol Biol Phys. 2002;54:1336–44.
10. Chen GP, Ahunbay E, Li XA. Automated computer optimization for 3D treatment planning of breast irradiation. Med Phys. 2008;35:2253–8.
11. Purdie TG, Dinniwell RE, Letourneau D, Hill C, Sharpe MB. Automated planning of tangential breast intensity-modulated radiotherapy using heuristic optimization. Int J Radiat Oncol Biol Phys. 2011;81:575–83.
12. Zhao X, Kong D, Jozsef G, Chang J, Wong EK, Formenti SC, Wang Y. Automated beam placement for breast radiotherapy using a support vector machine based algorithm. Med Phys. 2012;39:2536–43.
13. Purdie TG, Dinniwell RE, Fyles A, Sharpe MB. Automation and intensity modulated radiation therapy for individualized high-quality tangent breast treatment plans. Int J Radiat Oncol Biol Phys. 2014;90:688–95.
14. RaySearch Laboratories. RayStation 4.7 user manual RSL-D-61-242. Stockholm, Sweden: RSL; 2014.
15. Offersen BV, Boersma LJ, Kirkove C, Hol S, Aznar MC, Biete Sola A, Kirova YM, Pignol JP, Remouchamps V, Verhoeven K, Weltens C, Arenas M, Gabrys D, Kopek N, Krause M, Lundstedt

D, Marinko T, Montero A, Yarnold J, Poortmans P. ESTRO consensus guideline on target volume delineation for elective radiation therapy of early stage breast cancer. Radiother Oncol. 2015;114:3–10.
16. International Commission on Radiation Units and Measurements. Report 62: Prescribing, recording and reporting photon beam therapy (supplement to ICRU report 50). Bethesda: International Commission on Radiation Units and Measurements; 1999.
17. Fedorov A, Beichel R, Kalpathy-Cramer J, Finet J, Fillion-Robin JC, Pujol S, Bauer C, Jennings D, Fennessy F, Sonka M, Buatti J, Aylward S, Miller JV, Pieper S, Kikinis R. 3D Slicer as an image computing platform for the Quantitative Imaging Network. Magn Reson Imaging. 2012;30:1323–41.
18. International Commission on Radiation Units and Measurements. Report 83: Prescribing, recording, and reporting photon-beam intensity-modulated radiation therapy (IMRT). Bethesda: International Commission on Radiation Units and Measurements; 2010.
19. Smith BD, Bellon JR, Blitzblau R, Freedman G, Haffty B, Hahn C, Halberg F, Hoffman K, Horst K, Moran J, Patton C, Perlmutter J, Warren L, Whelan T, Wright JL, Jagsi R. Radiation therapy for the whole breast: executive summary of an American Society for Radiation Oncology (ASTRO) evidence-based guideline. Pract Radiat Oncol. 2018;8:145–52.
20. Cho BC, Mijnheer BJ, Bartelink H. Determining optimal two-beam axial orientations for heart sparing in left-sided breast cancer patients. Med Phys. 2004;31:111–21.
21. Ma C, Zhang W, Lu J, Wu L, Wu F, Huang B, Lin Y, Li D. Dosimetric comparison and evaluation of three radiotherapy techniques for use after modified radical mastectomy for locally advanced left-sided breast cancer. Sci Rep. 2015;5:12274.
22. Gopalakrishnan Z, Nair RK, Raghukumar P, Sarin B. Dosimetric comparison of treatment plans using physical wedge and enhanced dynamic wedge for the planning of breast radiotherapy. J Med Phys. 2018;43:46–51.
23. Zhang G, Jiang Z, Shepard D, Zhang B, Yu C. Direct aperture optimization of breast IMRT and the dosimetric impact of respiration motion. Phys Med Biol. 2006;51:357–69.
24. Nakamura N, Takahashi O, Kamo M, Hatanaka S, Endo H, Mizuno N, Shikama N, Ogita M, Sekiguchi K. Effects of geometrical uncertainties on whole breast radiotherapy: a comparison of four different techniques. J Breast Cancer. 2014;17:157–60.
25. Marks LB, Bentzen SM, Deasy JO, Kong FM, Bradley JD, Vogelius IS, El Naqa I, Hubbs JL, Lebesque JV, Timmerman RD, Martel MK, Jackson A. Radiation dose-volume effects in the lung. Int J Radiat Oncol Biol Phys. 2010;76:S70–6.
26. Taylor CW, Wang Z, Macaulay E, Jagsi R, Duane F, Darby SC. Exposure of the heart in breast cancer radiation therapy: a systematic review of heart doses published during 2003 to 2013. Int J Radiat Oncol Biol Phys. 2015;93:845–53.
27. Taylor C, Correa C, Duane FK, Aznar MC, Anderson SJ, Bergh J, Dodwell D, Ewertz M, Gray R, Jagsi R, Pierce L, Pritchard KI, Swain S, Wang Z, Wang Y, Whelan T, Peto R, McGale P. Estimating the risks of breast cancer radiotherapy: evidence from modern radiation doses to the lungs and heart and from previous randomized trials. J Clin Oncol. 2017;35:1641–9.
28. Pierce LJ, Feng M, Griffith KA, Jagsi R, Boike T, Dryden D, Gustafson GS, Benedetti L, Matuszak MM, Nurushev TS, Haywood J, Radawski JD, Speers C, Walker EM, Hayman JA, Moran JM. Recent time trends and predictors of heart dose from breast radiation therapy in a large quality consortium of radiation oncology practices. Int J Radiat Oncol Biol Phys. 2017;99:1154–61.
29. Kestin LL, Sharpe MB, Frazier RC, Vicini FA, Yan D, Matter RC, Martinez AA, Wong JW. Intensity modulation to improve dose uniformity with tangential breast radiotherapy: initial clinical experience. Int J Radiat Oncol Biol Phys. 2000;48:1559–68.
30. DeSantis CE, Ma J, Goding Sauer A, Newman LA, Jemal A. Breast cancer statistics, 2017, racial disparity in mortality by state. CA Cancer J Clin. 2017;67:439–48.
31. Borras JM, Lievens Y, Barton M, Corral J, Ferlay J, Bray F, Grau C. How many new cancer patients in Europe will require radiotherapy by 2025? An ESTRO-HERO analysis. Radiother Oncol. 2016;119:5–11.
32. Japanese Society for Radiation Oncology. Title of subordinate document. In: Japanese Structure Survey of Radiation Oncology in 2012 (First Report). Japanese Society for Radiation Oncology. 2012. https://www.jastro.or.jp/cmsdesigner/dlfile.php?entryname=aboutus_child&entryid=00048&fileid=00000002&/JASTRO_NSS_2012-01.pdf of subordinate document. Accessed 17 Aug 2018.